

# Well pattern-controlled heat transfer in in-situ oil shale conversion: a review of numerical modeling

Yu Cao<sup>(a)</sup>, Yi Pan<sup>(a)\*</sup>, Shuangchun Yang<sup>(a)</sup>, Hui Yang<sup>(b)</sup>

<sup>(a)</sup> College of Petroleum and Natural Gas Engineering, Liaoning Petrochemical University, Liaoning 113001, China

<sup>(b)</sup> Kunlun Safety & Health (Beijing) Technology Co. Ltd, Beijing 102200, China

Received 20 October 2025, accepted 1 July 2026, available online 3 August 2026

**Abstract.** *As an important alternative to conventional oil and gas resources, oil shale holds significant strategic importance. While in-situ conversion technology has addressed the challenges of deep oil shale mining, heat transfer efficiency remains the core bottleneck for its large-scale application. Through a systematic review of heat transfer simulation studies on oil shale in-situ conversion under well pattern control, this paper fills existing research gaps. It first systematically reviews the current research status of heat transfer during oil shale in-situ conversion, then clarifies the heat transfer mechanisms, and finally elaborates on the thermal-hydraulic-mechanical coupling model and research progress in in-situ extraction under well pattern control. It provides theoretical support for well pattern design and efficient mining in oil shale in-situ conversion projects.*

**Keywords:** *oil shale, well pattern, heat transfer characteristics, thermal-fluid-solid coupling, numerical simulation.*

## 1. Introduction

Global oil shale resources are extremely abundant, estimated at approximately  $1 \times 10^{13}$  t, equivalent to  $4.5 \times 10^{11}$  t of shale oil, which is four times the reserves of conventional petroleum resources [1]. Oil shale is a high-ash sedimentary rock rich in organic matter, from which shale oil produced by kerogen pyrolysis can be directly used as fuel or further processed to produce gasoline, diesel, and other fuels [2]. As an important alternative energy source, oil shale has attracted worldwide attention due to its vast reserves and comprehensive utilization value [3].

In-situ oil shale conversion technology still has certain limitations and drawbacks [4]. Generally, conduction heating is relatively mature in its

\* Corresponding author, [panyi\\_beijing@163.com](mailto:panyi_beijing@163.com)

process, simple, and easy to control, but it requires prolonged heating time and incurs high costs. Convection heating offers high heating efficiency, yet it results in significant heat loss and environmental damage. Radiation heating provides rapid heating rates; however, its heating range is constrained by technical limitations and remains in the research and development stage [5]. Reactive heating exhibits high efficiency and low cost, but its control process is complex. The in-situ pyrolysis of oil shale and hydrocarbon migration are influenced by multiple factors, making efficient heating a key challenge in the study of in-situ conversion technology [6]. Therefore, it is essential to clarify the heat transfer characteristics of oil shale under in-situ conversion conditions to provide a theoretical basis for the in-situ conversion process [7].

At present, a large number of scholars have studied the in-situ conversion technology of oil shale [8–10]. Based on the Web of Science database, a total of 726 articles from the past five years were analyzed using the search terms *oil shale*, *in situ conversion*, and *heat transfer*. As shown in Figure 1, recent research on in-situ pyrolysis of oil shale has primarily focused on fundamental mechanisms of oil shale pyrolysis, in-situ conversion technologies and reservoir engineering, and co-conversion techniques of oil shale. However, the heat transfer issue in in-situ oil shale conversion remains a critical bottleneck hindering its large-scale commercialization [11, 12]. Currently, there is a lack of comprehensive literature reviewing numerical simulation techniques for heat transfer in in-situ oil shale conversion under well pattern regulation. This paper fills the gap in literature.

This paper first describes the heat transfer characteristics of oil shale in-situ mining. Then, the solid heat transfer theory of oil shale in-situ conversion fluid is expounded, and the commonly used simulation software and thermal-fluid-solid coupling are introduced. Finally, the role of well pattern control in in-situ mining of oil shale is analyzed, the influence of well pattern on mining is discussed, and the numerical simulation and optimization directions of different well pattern models are discussed. The paper provides theoretical support and effective insights for the in-situ conversion development of oil shale and the optimization of well pattern deployment.

## **2. Current research status of in-situ heat transfer in oil shale conversion**

The key issue in the in-situ exploitation of oil shale lies in how external temperature can heat the ore layer to the effective pyrolysis temperature, which is essentially a matter of heat transfer characteristics. However, the underground environment is extremely complex, and different bedding structures may significantly affect the heat transfer characteristics of oil shale [13]. Heat conduction in an object occurs under the condition of no macroscopic relative displacement, where energy is transferred in the form of



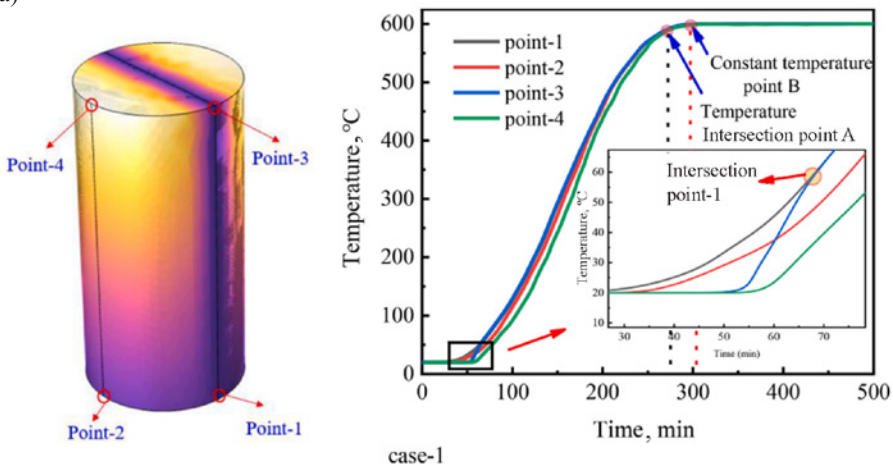
internal energy through the thermal motion of molecules or atoms constituting the object [14]. Convective heat transfer refers to the process of heat transfer that occurs when fluids of different temperatures undergo overall or partial relative movement. When an object's temperature is above absolute zero, the thermal motion of atoms and molecules continuously emits electromagnetic waves, releasing energy [15]. For heat transfer via conduction or convection, the presence of a medium is necessary, whereas radiative heat transfer can occur in a vacuum without requiring any medium [16].

Oil shale is a poor thermal conductor with low thermal conductivity, and it is a porous solid with relatively low porosity. Therefore, heat transfer issues inevitably arise during pyrolysis [17, 18]. These heat transfer mechanisms interact and overlap, making it highly challenging to comprehensively study the heat transfer behavior of oil shale during in-situ conversion process.

Regarding the key equipment for in-situ oil shale conversion, the large-scale spiral baffle downhole heater, Bu et al. [19] conducted numerical heat transfer simulations to analyze its performance under different heating powers and injected gas flow rates. At a gas flow rate of 160 m<sup>3</sup>/h and a heating power of 6 kW, the outlet temperature reached 280 °C. When  $h/\Delta p^{1/3}$  was used as the heat transfer performance indicator, the performance was optimal at 100 m<sup>3</sup>/h, most stable at 160 m<sup>3</sup>/h, and significantly affected by heating power at 200 m<sup>3</sup>/h, being approximately 6% lower than that at 100 m<sup>3</sup>/h. Gas heating was divided into three stages: rapid heating, stable heating, and excessive heating. The outlet temperature curve exhibited a two-stage variation due to the energy exchange balance between heating power and gas flow rate, preventing the outlet temperature from reaching the theoretical maximum. This large-scale heater can inject higher flow rates of heat-carrying gas, providing technical support for efficient in-situ pyrolysis of oil shale.

Regarding the thermo-hydro-mechanical (THM) coupling problem under high-temperature steam injection in oil shale, Jia et al. [20] investigated the heat transfer characteristics of Balikun oil shale from Xinjiang at temperatures

(a)



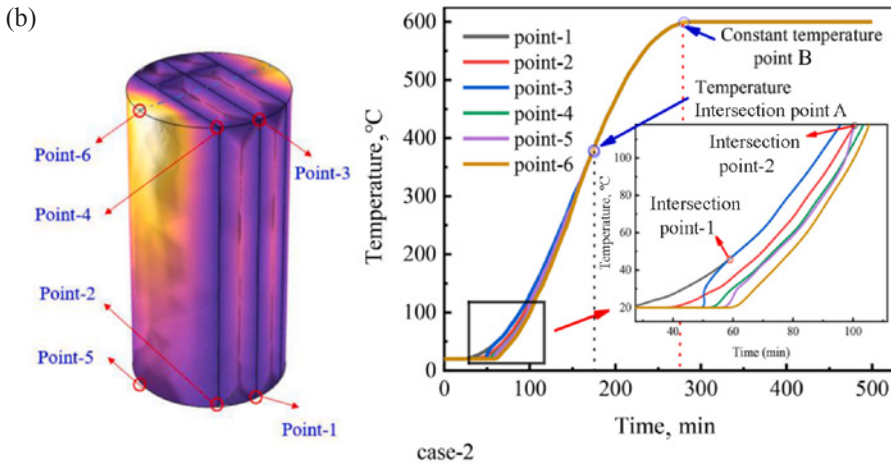


Fig. 2. Specimen temperature measurement points over time [20].

ranging from 25 to 550 °C. They demonstrated that a multi-fracture heating model provides a larger heating area compared to a single-fracture model, as shown in Figure 2, achieving a stable temperature of 600 °C 30 min earlier. The study revealed the permeability–heat transfer mechanism of oil shale during steam pyrolysis.

To further elucidate the evolution of the anisotropic thermal conductivity of oil shale with temperature and its correlation with anisotropic pore-fracture structures, Jin et al. [21] tested the weight loss, specific heat capacity, pore-fracture structure, and anisotropic thermal conductivity of oil shale with temperature. As shown in Figure 3, the main weight loss of oil shale occurs after 400 °C. The thermal conductivity of parallel and vertical beddings decreases

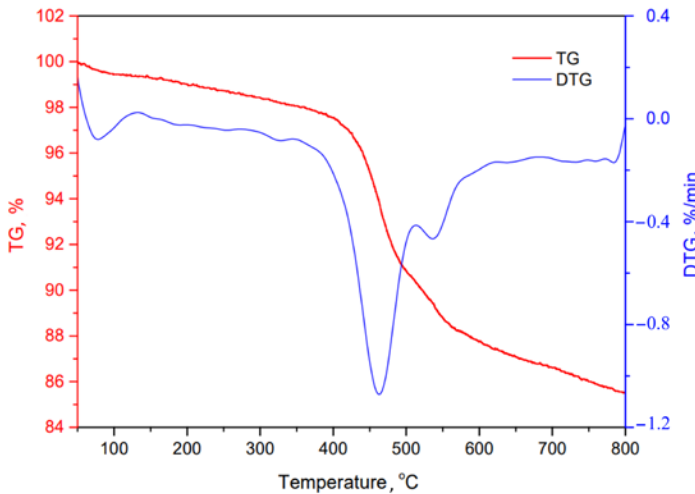


Fig. 3. TG and DTG curves of weight loss during oil shale pyrolysis [21].

linearly with the increase of temperature, and the thermal conductivity of parallel bedding is always greater than that of vertical bedding. The specific heat capacity increases first and then decreases, reaching a maximum at 400 °C. This study provides a key experimental basis for the optimization of oil shale in-situ pyrolysis mining technology.

Numerous scholars have conducted extensive research on heat transfer during in-situ oil shale conversion. Zhang et al. [22] established a spherical heat transfer model and a first-order heat transfer model, and suggested that heat transfer is an important factor affecting the yield of oil shale pyrolysis products. When the particle size of oil shale is small or the heating rate is slow, the calculation results of the first-order heat transfer model are more accurate. When the simulation is carried out in the same number of stages, the first-order heat transfer model can also reduce the computational load. Furthermore, regarding the heat transfer model within the pyrolysis reactor, Di Maio [23] used the discrete element method to simulate the heat transfer process of particles in the retort. The model considers the heat transfer between fluid and particles, particles and particles, fluid and reactor surface, and particles and reactor surface. The simulation results are in good agreement with the experimental data.

Overall, significant progress has been made in the field of heat transfer during in-situ oil shale conversion in recent years, particularly in multi-physics coupling simulations and a refined understanding of heat transfer processes. The core challenges faced by current research primarily stem from the geological characteristics of oil shale itself. Future research should focus on the low thermal conductivity characteristics of oil shale, deeply explore and optimize the heat transfer process, overcome the bottleneck of oil shale in-situ conversion technology, and enable its large-scale application.

### 3. Mechanism of heat transfer between fluids and solids in in-situ oil shale conversion

In the in-situ pyrolysis of oil shale, high-temperature gas brings heat from the gas injection well to the oil shale layer, and then the heat is transferred from the gas into the solid and liquid phases [24]. The numerical simulation of in-situ pyrolysis mining of oil shale requires establishing the corresponding physical model, and then calculating and solving the simulation results. The physical laws that the fluid must follow during flow are mainly the continuity equation, the mass conservation equation, and the motion equation [25].

The continuity equation is generally expressed as follows:

$$\frac{\partial \rho}{\partial t} + \nabla \cdot (\rho \vec{v}) = S_m, \quad (1)$$

where  $S_m$  denotes the mass source term.

If the established geometric model exhibits two-dimensional axisymmetric characteristics, the mass conservation equation is expressed as follows:

$$\frac{\partial \rho}{\partial t} + \frac{\partial}{\partial x}(\rho v_x) + \frac{\partial}{\partial r}(\rho v_r) + \frac{\rho v_r}{r} = S_m, \quad (2)$$

where  $x$  denotes the axial coordinate,  $r$  represents the radial coordinate,  $v_x$  indicates the axial velocity, and  $v_r$  stands for the radial velocity.

In an inertial reference frame, the motion equation can be expressed as follows:

$$\frac{\partial \rho}{\partial t}(\rho \vec{v}) + \nabla \cdot (\rho \vec{v} \vec{v}) = -\nabla p + \nabla \cdot (\bar{\bar{\tau}}) + \rho \vec{g} + \vec{F}, \quad (3)$$

where  $p$  denotes the fluid pressure,  $\rho \vec{g}$  represents the gravitational force,  $\vec{F}$  includes other external forces related to the model, and  $\bar{\bar{\tau}}$  signifies the stress tensor. The latter can be expressed as follows:

$$\bar{\bar{\tau}} = \mu \left[ (\nabla \vec{v} + \nabla \vec{v}^T) - \frac{2}{3} \nabla \cdot \vec{v} I \right], \quad (4)$$

where  $\mu$  denotes the molecular viscosity,  $I$  represents the unit tensor, and  $v$  indicates the swirl velocity.

If the established geometric model exhibits two-dimensional axisymmetric characteristics, the motion equations can be expressed as follows:

$$\begin{aligned} \frac{\partial}{\partial t}(\rho v_x) + \frac{1}{r} \frac{\partial}{\partial x}(r \rho v_x v_x) + \frac{1}{r} \frac{\partial}{\partial r}(r \rho v_r v_x) = -\frac{\partial p}{\partial x} \\ + \frac{1}{r} \frac{\partial}{\partial x} \left[ r \mu \left( 2 \frac{\partial v_x}{\partial x} - \frac{2}{3} (\nabla \cdot \vec{v}) \right) \right] + \frac{1}{r} \frac{\partial}{\partial r} \left[ r \mu \left( \frac{\partial v_x}{\partial r} + \frac{\partial v_r}{\partial x} \right) \right] + F_x, \end{aligned} \quad (5)$$

$$\begin{aligned} \frac{\partial}{\partial t}(\rho v_r) + \frac{1}{r} \frac{\partial}{\partial x}(r \rho v_x v_r) + \frac{1}{r} \frac{\partial}{\partial r}(r \rho v_r v_r) = -\frac{\partial p}{\partial r} + \frac{1}{r} \frac{\partial}{\partial x} \left[ r \mu \left( \frac{\partial v_r}{\partial x} + \frac{\partial v_x}{\partial r} \right) \right] \\ + \frac{1}{r} \frac{\partial}{\partial r} \left[ r \mu \left( 2 \frac{\partial v_r}{\partial r} - \frac{2}{3} (\nabla \cdot \vec{v}) \right) \right] - 2\mu \frac{v_r}{r^2} + \frac{2}{3} \mu (\nabla \cdot \vec{v}) + \rho \frac{v_z^2}{r} + F_r, \end{aligned} \quad (6)$$

$$\nabla \cdot \vec{v} = \frac{\partial v_x}{\partial x} + \frac{\partial v_r}{\partial r} + \frac{v_r}{r}. \quad (7)$$

Considering the energy model in the research process, heat transfer occurs when there is a temperature difference between different blocks. The heat conduction equation can be expressed as follows:

$$\rho \cdot C \frac{\partial T}{\partial t} = \nabla(\lambda \nabla T) + S(x, y, z, t). \quad (8)$$

The initial conditions can be expressed as follows:

$$T(x, y, z, 0) = T_0(x, y, z). \quad (9)$$

The boundary conditions can be expressed by the following three equations:

$$T|_{\Gamma_1} = T_w(x, y, z, t) (\Gamma \in \Gamma_1), \quad (10)$$

$$-\lambda \cdot \frac{\partial T}{\partial n} = q(x, y, z, t) (\Gamma \in \Gamma_2), \quad (11)$$

$$-\lambda \cdot \frac{\partial T}{\partial n} |_{\Gamma_3} = h(T - T_1) (\Gamma \in \Gamma_3). \quad (12)$$

In Equations (8)–(12),  $T(x, y, z, t)$  denotes the temperature field,  $\rho$  is the density of the material,  $\lambda$  represents the thermal conductivity,  $C$  is the specific heat capacity, and  $S(x, y, z, t)$  denotes the internal heat source generated by radiation.  $T_0(x, y, z)$  is the initial temperature distribution, while  $T_w(x, y, z, t)$  represents the prescribed temperature on the system boundary.  $q(x, y, z, t)$  denotes the heat flux density on the boundary, and  $h$  is the convective heat transfer coefficient.  $T_1$  represents the ambient temperature. The variables  $x, y, z$  denote the spatial coordinates and  $t$  denotes time.  $\nabla$  is the gradient operator and  $n$  represents the outward normal direction to the boundary.  $\Gamma_1$ ,  $\Gamma_2$ , and  $\Gamma_3$  denote the Dirichlet, Neumann, and Robin boundaries, respectively, of the computational domain.

In THM simulations of oil shale, software such as COMSOL or Ansys Fluent is commonly employed. COMSOL yields accurate results but is computationally demanding, while Fluent is more flexible and suited for larger-scale problems. When Fluent is utilized for such studies, it enables the simulation of heat conduction processes within both fluid and solid domains, as well as at their boundaries, requiring only the configuration of necessary parameters for the simulation.

The energy equation in Fluent is expressed as follows:

$$\frac{\partial}{\partial t}(\rho E) + \nabla \cdot (\vec{v}(\rho E + p)) = \nabla \cdot \left( k_{eff} \nabla T - \sum_j h_j \vec{J}_j + (\vec{\tau}_{eff} \cdot \vec{v}) \right) + S_h, \quad (13)$$

where  $E = h - \frac{p}{\rho} + \frac{v^2}{2}$ ,  $k_{eff}$  presents the effective conductivity, and  $\vec{J}$  denotes the diffusion flux.

Undeniably, oil shale is a typical porous medium characterized by low permeability and low porosity [26]. The energy conduction equation in Fluent is as follows:

$$\frac{\partial}{\partial t}(\rho h) + \nabla \cdot (\vec{v} \rho h) = \nabla \cdot (k \nabla T) + S_h. \quad (14)$$

In-situ underground pyrolysis of oil shale occurs in a multi-field coupled environment involving thermal, hydrodynamic, mechanical, and chemical interactions, representing a classic THM coupling problem in porous fractured rock

masses [27]. After the beginning of pyrolysis, the porosity and permeability of oil shale increase rapidly, which accelerates the seepage velocity of fluids and improves the diffusion rate of the temperature field. On the other hand, the density, elastic modulus, and Poisson's ratio of oil shale change with temperature, and the variation of the temperature field leads to the redistribution of stress field [28]. Ultimately, thermal stress modifies the apertures of pores and fractures, affecting the reservoir's porosity and permeability, which in turn induces further alterations in the seepage field. On the whole, the in-situ pyrolysis of oil shale is a thermal-flow-force multi-field dynamic coupling cycle process initiated by heat, involving changes in physical and chemical properties, and driving the evolution of permeability and seepage field through stress field adjustments.

Regarding shale gas extraction, Li et al. [29] developed a fully coupled multi-domain and multi-physics model, dividing the post-hydraulic fracturing shale reservoir into three core domains: SRD (stimulated reservoir domain), NSRD (non-stimulated reservoir domain), and HF (hydraulic fractures). The proposed THM coupling simulation accurately reflects the interactions of multi-domain and multi-physical processes during shale gas extraction.

For the pyrolysis of oil shale under microwave irradiation, Wang et al. [30] conducted numerical simulations based on a fully coupled electromagnetic-thermal-chemical-hydraulic model for three-dimensional porous media using the finite element method. As shown in Figure 4, high power was suitable for rapid heating, while low power facilitated efficient pyrolysis. Consequently, they proposed a variable-power heating mode, which simultaneously reduced heating time and improved thermal uniformity. Product analysis indicated that precise temperature control through parameter optimization was necessary to avoid secondary reactions of oil products. This study provides theoretical support for improving the heat transfer efficiency of microwave pyrolysis of oil shale.

Based on a fully coupled three-dimensional electro-thermal-chemical-fluid-solid model to study microwave heating in-situ conversion technology, Zhu et al. [31] found that the dielectric properties of oil shale are temperature-dependent, exhibiting a slow initial heating rate followed by rapid acceleration. When the pyrolysis temperature exceeds 500 °C, the heating rate increases significantly, and this phenomenon becomes more pronounced under high-power microwave irradiation. Compared to electric heating, microwave heating accelerates the generation of pressure gradients and thermal stress in oil shale while simultaneously enhancing its porosity and permeability. The research proves that microwave heating, rather than oil shale upgrading, has great potential.

In-situ oil shale conversion involves complex coupling of pyrolysis reactions, fluid flow, rock deformation, and heat transfer processes. The THM coupling model can simultaneously account for the interactions among temperature fields, seepage fields, and stress fields, thereby avoiding

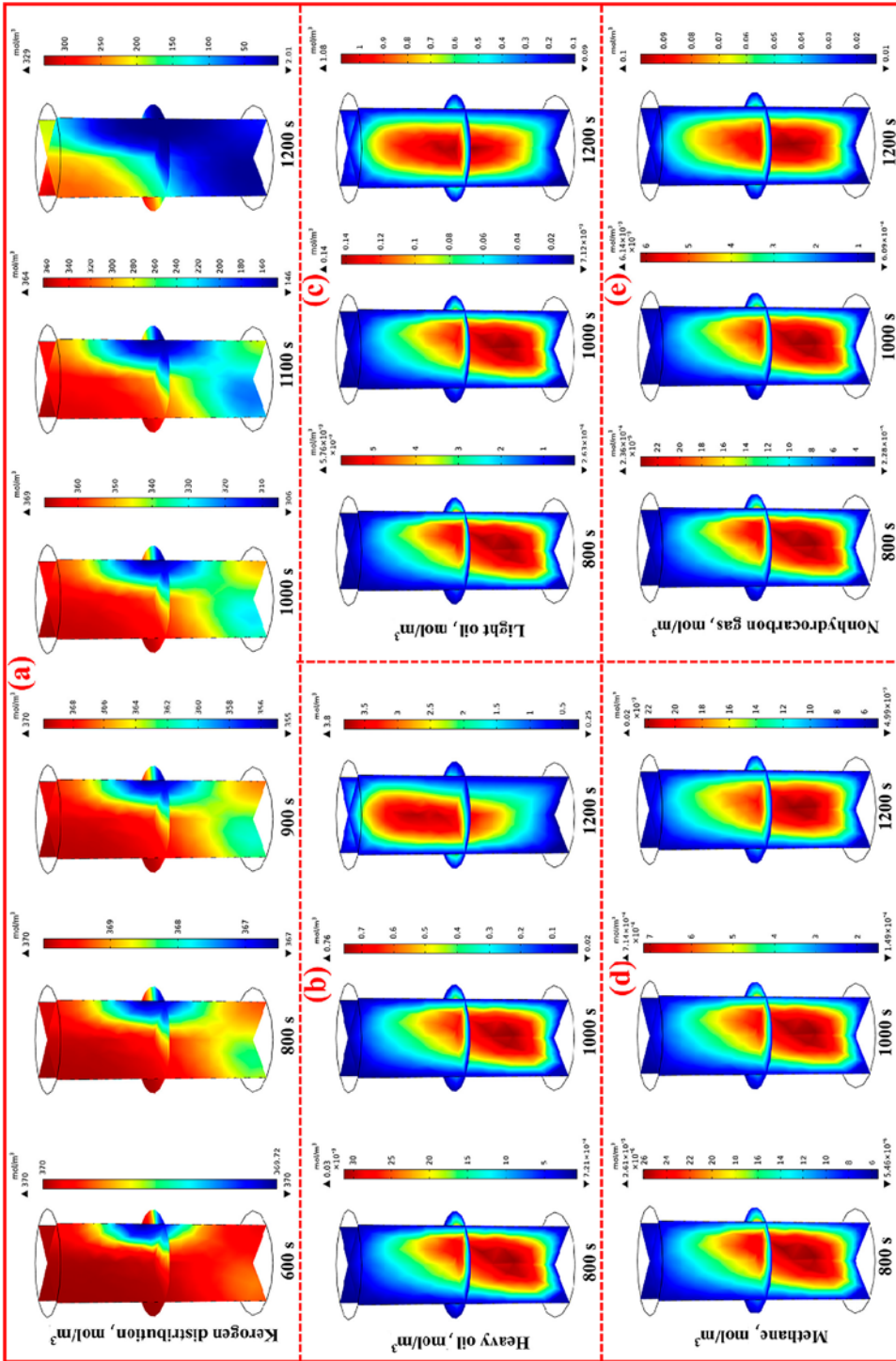


Fig. 4. Dynamic distribution of products during oil shale pyrolysis under a variable-power heating mode [30].

biases inherent in single-physics simulations [32]. Under well pattern control conditions, THM coupling simulations can analyze the impact of different operational parameters on heat transfer efficiency. THM coupling can simulate stress-strain field variations, predict formation change trends, and provide a basis for well pattern control strategies [33]. Therefore, conducting THM simulations for in-situ oil shale conversion serves as a critical approach to studying heat transfer mechanisms under well pattern control conditions.

#### **4. Numerical simulation of in-situ oil shale extraction via well pattern regulation**

The core of in-situ oil shale extraction lies in heating kerogen to pyrolyze it into oil and gas, a process that heavily relies on efficient heat transfer [34]. Under natural conditions, heat transfer in the formation is inefficient and difficult to control. Well pattern regulation establishes a controlled engineering system by deploying specific injection and production wells, fundamentally altering the heat transport environment. Specifically, well pattern control directly influences the temperature field distribution within the formation by adjusting the temperature, pressure, and flow rate of the injected fluid [35]. Large-scale field testing of well pattern control for heat transfer technology is usually difficult; therefore, numerical simulation has become an important tool for such studies.

Conducting numerical simulations of heat transfer in oil shale under well pattern control conditions is a key technical pathway to enhance the efficiency and safety of in-situ oil shale extraction [36]. The fundamental principle of well pattern control technology lies in precisely regulating the physical fields around the wellbore and within the reservoir to create an optimal environment for the pyrolysis and conversion of oil shale. The core concept of this technology involves meticulous management of injection and production wells to actively control the temperature, pressure, and fluid flow fields within the reservoir, thereby effectively guiding and constraining the oil shale pyrolysis process [37]. Its primary objective is to efficiently and safely convert solid oil shale kerogen into mobile hydrocarbon products within a controlled “reaction vessel” (i.e., the reservoir). Table 1 summarizes the well pattern deployment methods for in-situ oil shale extraction.

Numerical simulation serves as the cornerstone for the design and optimization of well pattern control technology. Researchers establish comprehensive mathematical models that couple heat transfer, chemical reactions, fluid flow, and rock mechanics to simulate and predict extraction performance under various well pattern control schemes [38].

**Table 1.** Well pattern deployment methods for in-situ oil shale extraction

Well pattern deployment type	Typical layout description	Advantages	Disadvantages
Five-spot/nine-spot well pattern	The center of a square area serves as an injection/heating well, with the four corners/edges as production wells	Established theoretical model, easy to manage, suitable for early small-scale pilot tests	Sweep efficiency may be non-uniform; poor adaptability to heterogeneous reservoirs; difficult to achieve large-scale volume heating
Triangular/hexagonal well pattern	Heating wells are arranged in an equilateral triangular or regular hexagonal array; production wells can be located at the center or edges of the array	Triangular: fast heating rate. Hexagonal: high energy utilization efficiency and uniform coverage	Requires a large number of wells, increasing investment costs; high requirements for drilling precision
Linear well pattern	Heating and production wells are arranged alternately in separate rows	Clear displacement direction, easy control of the heating sweep range, suitable for large-area development	High reservoir homogeneity required; prone to forming “dead oil zones” between well rows; limited lateral sweep efficiency
Vertical-horizontal well combination	Vertical and horizontal wells are deployed in coordination	Flexible layout, adjustable according to reservoir conditions	Complex design; requires precise geological understanding

The impact of well pattern on oil shale extraction is primarily reflected in two aspects: inter-well structure design and well spacing. Jia et al. [39] innovatively adopted an “injection well-heating hole-production well” configuration. By adding heating holes between injection and production wells, a low-temperature gas barrier was constructed to prevent groundwater intrusion into the production zone, thereby avoiding energy waste caused by direct exposure of groundwater to high temperatures in traditional well patterns. Simultaneously, this design allows nitrogen to heat up during flow, focusing thermal energy on hydrocarbon production rather than groundwater, which enhances pyrolysis efficiency and accelerates the initiation of oil production. Compared to conventional well patterns, this approach also reduces production delays and improves concurrent extraction efficiency.

In the investigation of a novel method for in-situ extraction of oil shale through long-distance horizontal wells high-temperature steam injection, Ren et al. [40] established a THM-coupled mathematical model that accounts for the anisotropy of oil shale. They compared the extraction efficiency between the conventional vertical well pattern and the new method, as illustrated in Figure 5. The results demonstrated that the new method achieves higher heating efficiency. Furthermore, key parameters were optimized, and economic analysis was conducted to validate the feasibility of the new approach, providing theoretical and data support for efficient in-situ pyrolysis of oil shale.

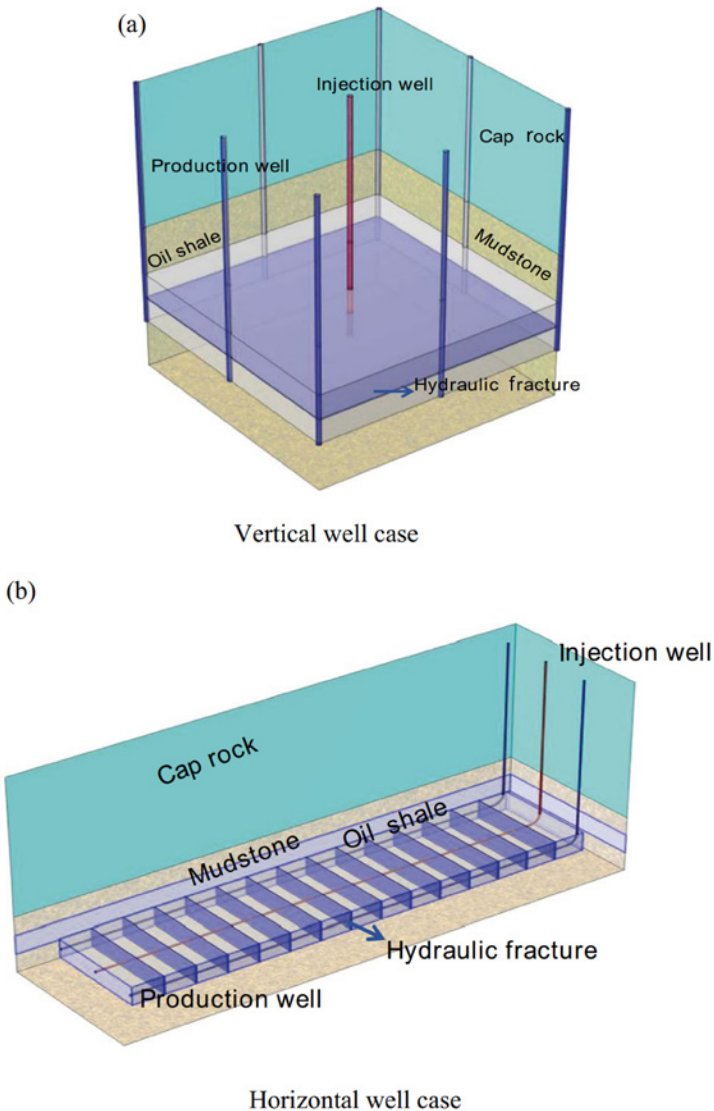


**Fig. 5.** Schematic diagram of vertical and horizontal well cases [40].

To explore low-power, high-yield three-dimensional oil shale well pattern models, Sun et al. [41] conducted numerical simulations using Ansys Fluent to evaluate the cumulative oil production, annual oil production, heating rate factor, and energy consumption per unit volume for the seven well pattern models shown in Figure 6. The results demonstrated that all models achieved in-situ pyrolysis directly without a preheating period. Model VII reached peak annual oil production at 360 days, with a peak heating rate factor of 3.696 at 540 days, and completed full pyrolysis by 780 days. Model VI exhibited the lowest energy consumption per unit volume at only 814.87 kW/m<sup>3</sup>, reducing consumption by 41.93% compared to other models and achieving the highest energy utilization efficiency. This study provides key technical support for the design of well types in in-situ oil shale mining field experiments.

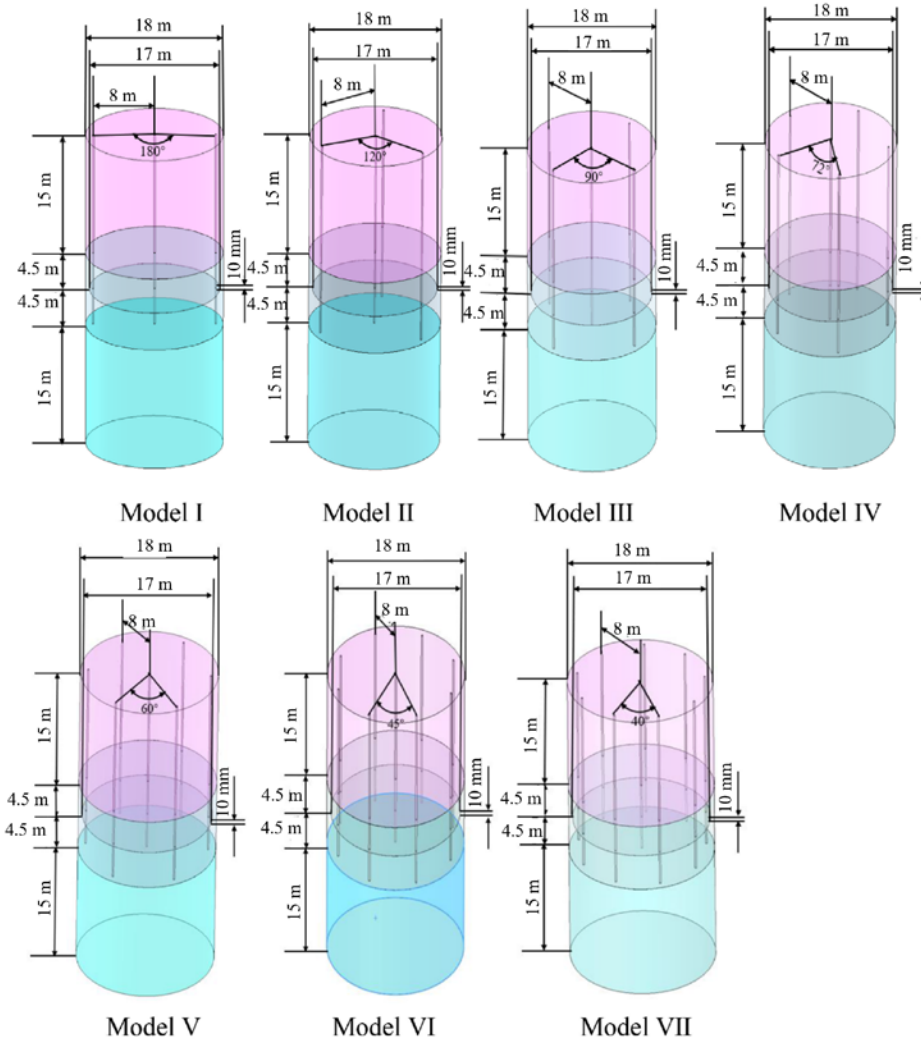


**Fig. 6.** Schematic diagram of different well pattern models for in-situ heating of oil shale [41].

At present, scholars mainly use the STARS module of CMG software to simulate the in-situ conversion and heating process of oil shale. Pei et al. [42] carried out numerical simulations of a seven-spot well group for nitrogen injection assisted in-situ conversion process (NAICP) and analyzed factors influencing the energy utilization rate and oil-gas recovery ratio. Under a gas injection temperature of 300 °C gas injection and a flow rate of 400 m<sup>3</sup>/day, the NAICP technology demonstrated higher production efficiency. The oil output equivalent and maximum oil yield were 1.17 and 1.28 times that of the in-situ conversion process, respectively, and energy utilization rate was improved. Song et al. [43] conducted numerical simulations of multi-level branch wells, showing that the injection temperature strongly influences hydrocarbon generation in oil shale. For multi-branch wells, a production scheme of five branch wells with a 60° branch angle and 40 m branch length achieved the highest oil and gas generation efficiency. These studies show that optimizing injection temperature and well structure can significantly improve oil production efficiency and energy utilization in the in-situ conversion of oil shale.

Current research has clearly revealed the complex effects of well spacing, well type, and well pattern on thermal field distribution, heating efficiency, and production dynamics. Future studies should adopt an economically oriented approach, focusing on establishing numerical simulation methods for well pattern control that account for multi-well pattern characteristics. This involves uncovering the synergistic mechanisms of thermal field regulation through well patterns and quantifying the differential effects of various well pattern combinations on the evolution of porosity and permeability parameter fields. The ultimate goal is to develop well group optimization technology that enhances heat transfer efficiency in self-generating heat in-situ conversion of oil shale, thereby providing theoretical support for predicting development outcomes and optimizing well pattern deployment.

## 5. Conclusions

This paper presents an in-depth examination of numerical simulation of well-pattern controlled heat conduction in in-situ oil shale conversion and draws the following conclusions:

1. The core of in-situ oil shale conversion lies in heat transfer efficiency. Current research has made progress in multi-field coupling simulations and understanding heat transfer mechanisms. However, the low thermal conductivity of oil shale leads to high costs and significant environmental risks. Well pattern control (including well type and spacing) directly affects the thermal field and extraction efficiency, making it a critical direction for optimization.

2. This paper fills a gap in the review of numerical simulations of in-situ heat transfer in oil shale under well pattern regulation. Future research should focus on refining the flow rate control ratio of production wells in group well regulation experiments, determining the optimal production flow ratio, and characterizing pyrolysis products, component variations, pyrolysis temperature, and its evolution patterns. These efforts aim to maximize pyrolysis oil yield and quality while optimizing the group well regulation extraction system.

This study provides valuable insights for the in-situ conversion and development of oil shale. Based on numerical simulation technology, it highlights the heat transfer mechanism in in-situ oil shale conversion and identifies new opportunities in the field under well pattern control.

### Data availability statement

No new data were generated or analyzed in support of this review.

### Acknowledgments

Yu Cao contributed to writing the original draft, Yi Pan contributed to funding acquisition, Shuangchun Yang contributed to supervision and proofreading, and Hui Yang was responsible for investigation and formal analysis. This work was supported by the National Science Foundation of China (project No. 52574041) Microscopic mechanism of transverse isotropic thermal damage in microwave-enhanced pyrolysis of oil shale. The publication costs of this article were partially covered by the Estonian Academy of Sciences.

### References

1. Al-Gharabli, S. I., Azzam, M. O. J., Al-Addous, M. Microwave-assisted solvent extraction of shale oil from Jordanian oil shale. *Oil Shale*, 2015, **32**(3), 240–251. <https://doi.org/10.3176/oil.2015.3.04>
2. Yihdego, Y., Salem, H. S., Kafui, B. G., Veljkovic, Z. Economic geology value of oil shale deposits: Ethiopia (Tigray) and Jordan. *Energy Sources Part A: Recovery, Utilization, and Environmental Effects*, 2018, **40**(17), 2079–2096. <https://doi.org/10.1080/15567036.2018.1488015>
3. Kong, D., Meng, X., Zhu, J., Zhou, W. Molecular dynamics simulation of surfactant induced wettability alteration of shale reservoirs. *Frontiers in Energy Research*, 2023, **11**, 1272132. <https://doi.org/10.3389/fenrg.2023.1272132>
4. Publisher's note. *Energy Reports*, 2022, **8**(S13), 1099–1112. <https://doi.org/10.1016/j.egy.2022.08.174>

5. Wang, L., Yang, D., Kang, Z., Zhao, J., Meng, Q. Experimental study on the effects of steam temperature on the pore-fracture evolution of oil shale exposed to the convection heating. *Journal of Analytical and Applied Pyrolysis*, 2022, **164**, 105533. <https://doi.org/10.1016/j.jaap.2022.105533>
6. Wang, L., Yang, D., Li, X., Zhao, J., Wang, G., Zhao, Y. Macro and meso characteristics of in-situ oil shale pyrolysis using superheated steam. *Energies*, 2018, **11**(9), 2297. <https://doi.org/10.3390/en11092297>
7. Bai, F., Sun, Y., Liu, Y., Guo, M. Evaluation of the porous structure of Huadian oil shale during pyrolysis using multiple approaches. *Fuel*, 2017, **187**, 1–8. <https://doi.org/10.1016/j.fuel.2016.09.012>
8. Kang, Z., Zhao, Y., Yang, D. Review of oil shale in-situ conversion technology. *Applied Energy*, 2020, **269**, 115121. <https://doi.org/10.1016/j.apenergy.2020.115121>
9. Hou, L., Tian, H., Yu, Z., Zhao, Z., Wu, S., Li, X. Dynamic evolution mechanism of reservoir physical properties during oil shale in situ conversion. *Energy & Fuels*, 2024, **38**(10), 8631–8640. <https://doi.org/10.1021/acs.energyfuels.4c00141>
10. Jiang, T., Yang, L., Zhu, C. Effect of pressure on the oil shale convection heating in-situ conversion process. *International Journal of Thermal Sciences*, 2025, **214**, 109940. <https://doi.org/10.1016/j.ijthermalsci.2025.109940>
11. Wang, C., Liu, Y., Song, D., Xu, J., Wang, Q., Zhang, S. Evaluation of bedding effect on the bursting liability of coal and coal-rock combination under different bedding dip angles. *Advances in Geo-Energy Research*, 2024, **11**(1), 29–40. <https://doi.org/10.46690/ager.2024.01.04>
12. Sun, Y., He, L., Kang, S., Guo, W., Li, Q., Deng, S. Pore evolution of oil shale during sub-critical water extraction. *Energies*, 2018, **11**(4), 842. <https://doi.org/10.3390/en11040842>
13. Liu, Z., Ma, H., Guo, J., Liu, G., Wang, Z., Guo, Y. Pyrolysis characteristics and effect on pore structure of Jimsar oil shale based on TG-FTIR-MS analysis. *Geofluids*, 2022, 7857239. <https://doi.org/10.1155/2022/7857239>
14. Wang, C.-Y. Measurements, mechanisms, and models of heat transport: by A. M. Hofmeister, Elsevier, 2018. *Contemporary Physics*, 2020, **61**(4), 303–304. <https://doi.org/10.1080/00107514.2020.1853240>
15. Mandal, I., Pal, S. COVID-19 pandemic persuaded lockdown effects on environment over stone quarrying and crushing areas. *Science of The Total Environment*, 2020, **732**, 139281. <https://doi.org/10.1016/j.scitotenv.2020.139281>
16. Metwally, H., Mahmoud, N. A., Aboelsoud, W., Ezzat, M. Yearly performance of the photovoltaic active cooling system using the thermoelectric generator. *Case Studies in Thermal Engineering*, 2021, **27**, 101252. <https://doi.org/10.1016/j.csite.2021.101252>
17. Pan, Y., Jia, Y., Zheng, J., Yang, S., Bttina, H. Research progress of fracture development during in-situ cracking of oil shale. *Journal of Analytical and Applied Pyrolysis*, 2023, **174**, 106110. <https://doi.org/10.1016/j.jaap.2023.106110>

18. Jiang, H., Liu, S., Wang, J., You, Y., Yuan, S. Study on evolution mechanism of the pyrolysis of Chang 7 oil shale from Ordos basin in China. *Energy*, 2023, **272**, 127097. <https://doi.org/10.1016/j.energy.2023.127097>
19. Bu, Q., Li, Q., Li, X. Numerical heat transfer simulation of oil shale large-size downhole heater. *Applied Sciences*, 2024, **14**(6), 2235. <https://doi.org/10.3390/app14062235>
20. Jia, Y., Huang, X., Yang, D., Sun, D., Luo, C. Thermo-hydro-mechanical coupling in oil shale: investigating permeability and heat transfer under high-temperature steam injection. *Case Studies in Thermal Engineering*, 2024, **61**, 104862. <https://doi.org/10.1016/j.csite.2024.104862>
21. Jin, J., Liu, J., Jiang, W., Cheng, W., Zhang, X. Evolution of the anisotropic thermal conductivity of oil shale with temperature and its relationship with anisotropic pore structure evolution. *Energies*, 2022, **15**(21), 8021. <https://doi.org/10.3390/en15218021>
22. Zhang, F., Parker, J. C. An efficient modeling approach to simulate heat transfer rate between fracture and matrix regions for oil shale retorting. *Transport in Porous Media*, 2010, **84**, 229–240. <https://doi.org/10.1007/s11242-009-9495-x>
23. Di Maio, F. P., Di Renzo, A., Trevisan, D. Comparison of heat transfer models in DEM-CFD simulations of fluidized beds with an immersed probe. *Powder Technology*, 2009, **193**(3), 257–265. <https://doi.org/10.1016/j.powtec.2009.03.002>
24. Wang, L., Yang, D., Zhang, Y., Li, W., Kang, Z., Zhao, Y. Research on the reaction mechanism and modification distance of oil shale during high-temperature water vapor pyrolysis. *Energy*, 2022, **261**, 125213. <https://doi.org/10.1016/j.energy.2022.125213>
25. Wang, X., Huang, L., Li, X., Bi, S., Li, H., Zhang, J. et al. Wellbore multiphase flow behaviors of gas kick in deep water horizontal drilling. *Frontiers in Physics*, 2022, **10**, 1049547. <https://doi.org/10.3389/fphy.2022.1049547>
26. Wu, Z., Fang, F., Li, X., Xiao, H., Liu, X., Rao, Y. et al. Division method and seepage law of seepage channels in a tight reservoir. *Geofluids*, 2021, 4804513. <https://doi.org/10.1155/2021/4804513>
27. Huang, H., Yu, H., Xu, W., Lyu, C., Micheal, M., Xu, H. et al. A coupled thermo-hydro-mechanical-chemical model for production performance of oil shale reservoirs during in-situ conversion process. *Energy*, 2023, **268**, 126700. <https://doi.org/10.1016/j.energy.2023.126700>
28. Yin, T., Wu, Y., Li, Q., Wang, C., Wu, B. Determination of double-K fracture toughness parameters of thermally treated granite using notched semi-circular bending specimen. *Engineering Fracture Mechanics*, 2020, **226**, 106865. <https://doi.org/10.1016/j.engfracmech.2019.106865>
29. Li, W., Liu, J., Zeng, J., Leong, Y.-K., Elsworth, D., Tian, J. et al. A fully coupled multidomain and multiphysics model for evaluation of shale gas extraction. *Fuel*, 2020, **278**, 118214. <https://doi.org/10.1016/j.fuel.2020.118214>
30. Wang, H., Li, X., Zhu, J., Yang, Z., Zhou, J., Yi, L. Numerical simulation of oil shale pyrolysis under microwave irradiation based on a three-dimensional

- porous medium multiphysics field model. *Energies*, 2022, **15**(9), 3256. <https://doi.org/10.3390/en15093256>
31. Zhu, J., Yi, L., Yang, Z., Duan, M. Three-dimensional numerical simulation on the thermal response of oil shale subjected to microwave heating. *Chemical Engineering Journal*, 2021, **407**, 127197. <https://doi.org/10.1016/j.cej.2020.127197>
  32. Chen, X., Rao, X., Xu, Y., Liu, Y. An effective numerical simulation method for steam injection assisted in situ recovery of oil shale. *Energies*, 2022, **15**(3), 776. <https://doi.org/10.3390/en15030776>
  33. Liu, Y., Xue, L., Bai, F., Zhao, J., Yan, Y. Three-dimensional numerical simulation of hydrocarbon production and reservoir deformation of oil shale in situ conversion processing using a downhole burner. *ACS Omega*, 2022, **7**(27), 23695–23707. <https://doi.org/10.1021/acsomega.2c02317>
  34. Ramsay, T. Uncertainty quantification of an explicitly coupled multiphysics simulation of in-situ pyrolysis by radio frequency heating in oil shale. *SPE Journal*, 2020, **25**(3), 1443–1461. <https://doi.org/10.2118/200476-PA>
  35. Lu, Y.-C., Song, S.-R., Taguchi, S., Wang, P.-L., Yeh, E.-C., Lin, Y.-J. et al. Evolution of hot fluids in the Chingshui geothermal field inferred from crystal morphology and geochemical vein data. *Geothermics*, 2018, **74**, 305–318. <https://doi.org/10.1016/j.geothermics.2017.11.016>
  36. Yu, H., Tang, J., Zhang, X., Ren, L., Zhang, X. Analysis of effective pyrolysis zone and heat loss in oil shale reservoir with random fractures. *ACS Omega*, 2023, **8**(48), 45687–45699. <https://doi.org/10.1021/acsomega.3c06014>
  37. Nie, B. Study on thermal decomposition of oil shale: two-phase fluid simulation in wellbore. *Energy*, 2023, **272**, 127124. <https://doi.org/10.1016/j.energy.2023.127124>
  38. Briceño Montilla, M. J., Li, S., Zhang, Z., Hu, Y., He, J., Bo, Z. et al. Energy recovery analysis through numerical simulations of steam injection in continental shale oil reservoirs. *Journal of Petroleum Exploration and Production Technology*, 2025, **15**, 69. <https://doi.org/10.1007/s13202-025-01970-4>
  39. Jia, B., Huang, Z. Oil shale in situ production using a novel flow-heat coupling approach. *ACS Omega*, 2024, **9**(7), 7705–7718. <https://doi.org/10.1021/acsomega.3c07009>
  40. Ren, S., Jia, Y., Zhao, J., Yang, D., Wang, G. Numerical study on in-situ mining oil shale by high-temperature steam injection in long-distance horizontal wells. *Geomechanics and Geophysics for Geo-Energy and Geo-Resources*, 2024, **10**, 161. <https://doi.org/10.1007/s40948-024-00869-4>
  41. Sun, T., Liu, H., Zhang, Y., Li, Y. Numerical simulation and optimization study of in-situ heating for three-dimensional oil shale exploitation with different well patterns. *Case Studies in Thermal Engineering*, 2024, **55**, 104089. <https://doi.org/10.1016/j.csite.2024.104089>
  42. Pei, S., Wang, Y., Zhang, L., Huang, L., Cui, G., Zhang, P. et al. An innovative nitrogen injection assisted in-situ conversion process for oil shale recovery:

- mechanism and reservoir simulation study. *Journal of Petroleum Science and Engineering*, 2018, **171**, 507–515. <https://doi.org/10.1016/j.petrol.2018.07.071>
43. Song, X., Zhang, C., Shi, Y., Li, G. Production performance of oil shale in-situ conversion with multilateral wells. *Energy*, 2019, **189**, 116145. <https://doi.org/10.1016/j.energy.2019.116145>